ACS APPLIED MATERIALS & INTERFACES

Research Article

www.acsami.org

Polythiophene-*g*-poly(ethylene glycol) with Lateral Amino Groups as a Novel Matrix for Biosensor Construction

Huseyin Akbulut,[†] Guliz Bozokalfa,[‡] Duygu N. Asker,[‡] Bilal Demir,[‡] Emine Guler,[‡,§] Dilek Odaci Demirkol,[‡] Suna Timur,*[,‡,§] and Yusuf Yagci*[,†,∥]

[†]Istanbul Technical University, Department of Chemistry, Faculty of Science and Letters, Istanbul, Turkey

[‡]Ege University Faculty of Science Biochemistry Department 35100 Bornova-Izmir, Turkey

[§]Ege University, Institute of Drug Abuse Toxicology & Pharmaceutical Sciences, 35100 Bornova, Izmir, Turkey

[∥]Center of Excellence for Advanced Materials Research (CEAMR) and Chemistry Department Faculty of Science, King Abdulaziz University, P.O. Box 80203, Jeddah 21589, Saudi Arabia

Supporting Information

ABSTRACT: In the ever-expanding field of conducting polymer research, functionalized graft hybrid copolymers have gained considerable interest in the biomedical engineering and biosensing applications, particularly. In the present work, a new biosensor based on conducting graft copolymer for the detection of phenolic compounds was developed. Thereby, a robust and novel material, namely "polythiophene-*g*-poly(ethylene glycol) with lateral amino groups" (PT-NH_2-*g*-PEG) hybrid conducting polymer was synthesized via Suzuki condensation polymerization and characterized with ^{1}H NMR analysis, UV−vis spectroscopy, gel permeation chromatography (GPC) and fluorescence spectroscopy. PT-NH_2-*g*-PEG architecture was then applied as an immobilization matrix to accomplish extended biosensing function. In a typical process, Laccase was utilized as a model enzyme for the detection of phenolic compounds. Detailed surface characterization of PT-NH_2-*g*-PEG/Lac was performed by cyclic voltammetry, electrochemical impedance spectroscopy, atomic force microscopy, fluorescence microscopy and scanning electron microscopy measurements. Optimum pH and polymer amount were found to be pH 6.5 and 0.5 mg polymer, respectively, with the linear range of 0.0025−0.05 mM and 132.45 μA/mM sensitivity. The kinetic parameters of PT-NH_2-*g*-PEG/Lac are 0.026 mM for K_m^{app} and 7.38 μA for I_{max}, respectively. Furthermore, the PT-NH_2-*g*-PEG/Lac biofilm was retained 82% of its activity for 12 days indicating excellent recovery as tested with artificial wastewater.

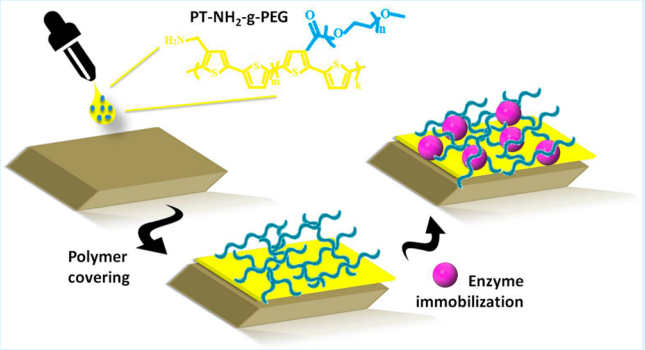

KEYWORDS: *conducting polymers, graft copolymer, polythiophene, poly(ethylene glycol), surface modification, biomolecule immobilization, biosensor*

INTRODUCTION

There exists a wide variety of organic materials that are developed to be used in many biological processes. These materials include synthetic polymers, ceramics, carbonated structures, tissue- or cell-derived natural polymers, and composites made from variety combinations of such materials.[1,2] Apart from many functional organic materials, conducting polymers (CPs) have presented great potential in the area of sensors, anticorrosion coatings, batteries, capacitors, actuators and optical devices.[3,4] These types of polymers (also known as electro-active conjugated polymers) illustrate tremendous conductivity and mechanical strengths and processability. By taking into consideration of the excellent properties of CPs, they have been used as an immobilization matrix to generate a supportive layer in biosensing applications. To create a stable and cost-effective immobilization platform, several immobilization strategies such as noncovalent interactions (physical adsorption, electrostatic assembly, hydrophobic interactions) or covalent binding of biological element have been developed.[5−9]

Among various electro-active conjugated polymers, polyenes and polyaromatics like polyaniline (PAn), polypyrrole (PPy), polythiophene (PT), poly(p-phenylene), poly(phenylenevinylene) (PPV) classes have been extensively investigated in chemical sensing applications.[10] Advances in the field of bioimaging have profoundly impacted the use of water-soluble biopolymers. Intensive research activity has focused on the development of fluorescence-based water-soluble organic conjugated polymers relying on π-electron delocalization features.[11] Among the vast number of π-

Received: June 5, 2015
Accepted: September 1, 2015
Published: September 1, 2015

DOI: 10.1021/acsami.5b04967
ACS Appl. Mater. Interfaces 2015, 7, 20612−20622

conjugated polymers, PTs and its derivatives are the most promising polymer in terms of relatively good electrochemical, electrochromic, luminescent, and shielding properties.[12,13] Water solubility, primary essential requirement in biological process, relies on the existence hydrophilic supports such as poly(ethylene glycol) (PEG), which comes to the forefront from a highly versatile class of polyethers. PEG combines excellent solubility in both water and organic solvents with biocompatibility. These materials exhibit no antigenicity, immunogenicity, or toxicity and are consumed in human body as approved by the U.S. American Food and Drug Administration.[11,14,15]

Phenolic compounds are the waste products of current industrial activity relevant to water, sewage, soil and even food. Phenolic compounds are also known as toxic structures to the most living organism. Concomitantly, their toxicity increases owing to their poor biodegradability.[16] Nowadays, there are some developed technical standards to determine phenolics such as colorimetric, gas and liquid chromatography, capillary electrophoresis, and their variations.[17] Even though, conventional standardized techniques enable accurate data for the estimation of several phenolic compounds, these approaches are highly expensive and time-consuming. As a consequence, novel strategies for the detection of phenolic compounds are needed. Within this framework, enzymatic biosensors are manifested as a promising technology via many advantages like being portable, cost-effective and facile determination of the phenolic structures.[18]

Until now, laccase (Lac), tyrosinase, and peroxidase biosensors have gained popularity in the determination of phenolic compounds. Among these three enzymes, Lac biosensors have gained more attraction and used to combine to various biodetecting platforms. Lac immobilization was established to analyze various phenolic compounds via direct adsorption, covalent binding, entrapment in polymeric gels or membranes and cross-linking processes. Recently, a number of new support matrices, namely epoxy resin membranes,[19] multiwalled carbon nanotube (CNT) paste electrodes,[20] chitosan/CNT nanocomposites,[21] pyrenehexanoic acid-modified hierarchical carbon microfibers/CNT composites,[22] poly(vinyl alcohol) photopolymers,[23] diglycerylsilane sol−gel matrix,[24] self-assembled monolayers of 3-mercaptopropionic acid[25] and quantum dot modified gold surfaces,[26] polyethylenimine coated gold nanoparticle modified glassy carbon electrodes (GCEs),[27] and multiwalled CNTs/PPy electrodeposited platinum electrodes[28] have been developed. In a recent report, Songurtekin et al. constructed a Lac biosensor by using newly synthesized histidine intercalated montmorillonite clay minerals and successfully applied for the analysis of phenolics.[29]

Herein, we describe a novel Lac biosensor where polythiophene-NH_2-*g*-poly(ethylene glycol) (PT-NH_2-*g*-PEG) conducting polymer was used as immobilization platform. After the polymer was drop-coated on the graphite electrode (GE), surface characterization was performed by using various techniques such as electrochemical techniques, microscopy, and so on. Lac immobilization was carried out by cross-linking of the enzyme on PT-NH_2-*g*-PEG via glutaraldehyde (GA) through pendant amino groups present in the structure. Prior to sample application, electrochemical biosensor characteristics were investigated by using catechol as a model phenolic compound.

2. EXPERIMENTAL SECTION

Materials. Laccase (Lac; EC 1.10.3.2, from *Agaricus bisporus*, 8.85 Unit/mg) was obtained from Biochemika. Catechol, glutaraldehyde (GA) solution (25%, v/v), phenol, ascorbic acid, uric acid, 3-acetamidophenol, tetrahydrofuran (THF), tetrakis (triphenylphosphine) palladium(0) ($Pd(PPh_3)_4$), thiophene-3-carboxylic acid, thiophen-3-ylmethanol, phosphorus tribromide (PBr_3), *N*-bromosuccinimide (NBS), 4-(*N*,*N*′-dimethyl) amino pyridine (DMAP), dicyclohexylcarbodiimide (DCC), poly(ethylene glycol) mono methyl ether (PEG_{2000}), phthalimide potassium salt and hydrazine monohydrate (98%), 2,5-thiophenediboronic acid were purchased from Sigma-Aldrich. Ethanol was purchased from MERCK. All other reagents used were of analytical grade.

Measurements. ^{1}H NMR spectra were performed with an Agilent VNMRS 500 MHz, and chemical shifts were recorded in ppm units using tetramethylsilane as an internal standard. UV/vis absorbance measurements were recorded on a Shimadzu UV-1601 spectrometer. Fluorescence measurements were performed with a model LS-50 spectrometer from PerkinElmer at room temperature. Gel-permeation chromatography (GPC) measurements were carried out in Viscotek GPCmax auto sampler system. Instrument was equipped with a pump (GPCmax, Viscotek Corp., Houston, TX), light-scattering detector (λ_0 = 670 nm, Model 270 dual detector, Viscotek Corp.) consisting of two scattering angles: 7° and 90° and the refractive (RI) index detector (VE 3580, Viscotek Corp.). Both detectors were calibrated with PS standards in the narrow molecular weight distribution. Three ViscoGEL GPC columns (G2000HHR, G3000HHR and G4000HHR) employed with THF in the 1.0 mL min^{-1} flow rate at 30 °C. All data were analyzed using Viscotek OmniSEC Omni-01 software.

*Synthesis of 2,5-Dibromothiophene-3-carboxylic acid (**1**).* Thiophene-3-carboxylic acid (2g, 15.6 mmol) and NBS (6.4 g, 35.9 mmol) were added to dry 50 mL of DMF under nitrogen atmosphere. The solution was stirred at 50 °C under nitrogen for 24 h. The reaction mixture was washed with brine. After that, the aqueous layer was extracted with CH_2Cl_2 and the organic layers were combined, dried over Na_2SO_4 and concentrated under reduced pressure to yield 1 (2.6 g, 60%, white powder). ^{1}H NMR (d-DMSO, 500 MHz): δ 7.43 (s, 1H), 13.32 (s, 1H), (Supporting Information, Figure S1).

Synthesis of Dibromothiophene-Functional PEG Macromonomers (DBT-PEG). 2,5-Dibromothiophene-3-carboxylic acid (**1**) (4.1 g, 14.3 mmol), DMAP (174.7 mg, 1.43 mmol), Me-PEG_{2000}−OH (25.74 g, 12.87 mmol) were dissolved in 100 mL of dry CH_2Cl_2 under nitrogen atmosphere. To this solution was added DCC (3.246 g, 15.7 mmol) in 20 mL dry CH_2Cl_2 dropwise under nitrogen. Then, the reaction mixture was stirred for 5 days at room temperature. After that, the mixture was filtered and washed with 250 mL of CH_2Cl_2. The organic phase was quenched with 10% $NaHCO_3$ and brine, and then dried over Na_2SO_4. The solution was concentrated and passed through a silica-gel column using CH_2Cl_2 as eluent. After removal of solvent in vacuo, the polymer was precipitated in cold diethyl ether and dried to yield DBT-PEG (18 g, 85%, white powder). ^{1}H NMR ($CDCl_3$, 500 MHz): δ 3.85−3.46 (broad), 3.38 (broad), 7.34 (s, 1H), (Supporting Information, Figure S2).

*Synthesis of (2,5-Dibromothiophen-3-yl)methanol (**2**).* To the solution of thiophen-3-ylmethanol (6.45 g, 56.5 mmol), in 180 mL of dry THF, NBS (22.13 g, 12.42 mmol) was drop-wisely added and stirred for 3 days at room temperature under nitrogen atmosphere. The solvent was evaporated in vacuo. Then, the remaining crude material was washed with KOH (1.0 M, 30 mL), extracted with diethyl ether and purified by flash column chromatography (SiO_2, hexan/ethyl acetate = 4:1, as eluent) to yield 2 (6.4 g, 41% brown oil). ^{1}H NMR ($CDCl_3$, 500 MHz): δ 1.91 (broad, 1H), 4.55 (s, 2H), 7,0 (s, 1H), (Supporting Information, Figure S3).

*Synthesis of 2,5-Dibromo-3-(bromomethyl)thiophene (**3**).* To the solution of **2** (6.4 g, 23.52 mmol), in 30 mL of dry CH_2Cl_2 at 0 °C under nitrogen atmosphere, PBr_3 (4.5 mL, 47.88 mmol) was added drop-wise and stirred at room temperature under nitrogen atmosphere for 24 h. Then, the solvent was evaporated in vacuo and oil residue

DOI: 10.1021/acsami.5b04967
ACS Appl. Mater. Interfaces 2015, 7, 20612−20622

treated with $NaHCO_3$ (30 mL, 10%) at 0 °C and extracted with CH_2Cl_2. The organic layer was evaporated and purified by flash column chromatography (SiO_2, hexan) to yield 3 (5.6 g, 71%, white solid). ^1H NMR ($CDCl_3$, 500 MHz): δ 4.38 (s, 2H), 6.99 (s, 1H), (Supporting Information, Figure S4).

Synthesis of 2-((2,5-Dibromothiophen-3-yl)methyl)isoindoline-1,3-dione (4). To the solution of **3** (4.0 g, 12 mmol) in 10 mL of dry DMF, potassium phthalimide (3.3 g, 18 mmol) were added. After stirring for 24 h at 160 °C in a Schleck tube under nitrogen atmosphere, the reaction mixture was poured into water. The precipitate was washed with water, purified by flash column chromatography (SiO_2, CH_2Cl_2), precipitated in ethanol and dried under vacuum to yield 4 (3.2 g, 66%, white solid). ^1H NMR ($CDCl_3$, 500 MHz): δ 4.77 (s, 2H), 6.99 (s, 1H), 7.93–7.69 (m, 2H), (Supporting Information, Figure S5).

Synthesis of (2,5-dibromothiophen-3-yl)methanamine (MA-DBT). The solution of **4** (3.2 g, 7.98 mmol) in 150 mL of absolute ethanol with 25 mL of hydrazine were stirred at 90 °C for 5 h in a Schlenck tube. After allowing to cool to room temperature, the solvent was evaporated in vacuo and residue treated with $NaHCO_3$ (50 mL, 10%) and extracted with CH_2Cl_2 to yield MA-DBT (0.5 g, 74%, yellow oil). ^1H NMR ($CDCl_3$, 500 MHz): δ 2.35–1.94 (m, 2H), 3.74 (s, 2H), 6.95 (s, 2H), (Supporting Information, Figure S6).

Synthesis of Polythiophene with Primary Amine and PEG Side Groups (PT-NH_2-g-PEG). The reaction solution was prepared with 30 mL of THF and 20 mL of aqueous 2.0 M K_2CO_3 solution under nitrogen. Prior to use, this solution was degassed by bubbling nitrogen over a period of 30 min. In the 10 mL of the reaction solution, MA-DBT (0.81 g, 3.0 mmol), DBT-PEG (2.3 g, 1.0 mmol), 2,5-thiophenediboronic acid (0.704 g, 4.1 mmol), $Pd(PPh_3)_4$) (0.092 g, 0.08 mmol) was dissolved in a Schlenk tube under nitrogen. The reaction mixture was freed from air by freeze–thaw technique and then stirred at 70 °C for 4 days under vacuum. After stirring, the reaction mixture was extracted with CH_2Cl_2 and small amount of water. The organic phase was concentrated and precipitated in excess diethyl ether to yield PT-NH_2-g-PEG (1.57 g, white powder). ^1H NMR ($CDCl_3$, 500 MHz): δ 1.94–1.65 (broad), 3.38 (broad), 3.45–3.8 (broad), 7.58–7.01 (broad).

Biosensor Fabrication. Initially, the GE was polished on wet emery paper and rinsed with distilled water. Afterward, 1.0 mg of PT-NH_2-g-PEG was dissolved in 2.0 mL of a sodium phosphate buffer (50 mM, pH 6.5)/THF (19:1 v/v) mixture. To construct the modified electrode, we mixed 5.0 μL of the PT-NH_2-g-PEG solution (0.5 mg/mL), 1.0 mg of Lac (2.5 μL in sodium phosphate buffer (50 mM, pH 6.5) and 2.5 μL of GA (2.5% in sodium phosphate buffer (50 mM, pH 6.5)) and dropped onto the electrode and allowed to dry at ambient conditions for 90 min. Prior to measurements, the electrode surface was rinsed with distilled water to eliminate the unbounded residues.

Surface Characterization. Cyclic voltammetry (CV) measurements were performed to investigate oxidation and reduction current peaks in the potential range of 0.005–0.2 V, in the presence of 5.0 mM $[Fe(CN)_6]^{3-/4-}$ as redox probe and 1.0 mM KCl as supporting electrolyte. Electrochemical impedance spectroscopy (EIS) measurements were performed in sodium phosphate buffer (50 mM, pH 6.0) in the presence of 5.0 mM, $[Fe(CN)_6]^{3-/4-}$ and 0.1 M KCl with a frequency range from 0.03 to 1000 Hz at 0.18 V. CV and chronoamperometric measurements were carried out with a PalmSens Potentiostat (Palm Instruments, Houten, Netherlands). A CHI 6005C electrochemical analyzer (CH Instruments Incorporation, Austin, TX) was utilized for the EIS analysis.

Upon electrochemical characterization, microscopic techniques were used to prove surface modification. Morphology of the modified surface was imaged by scanning electron microscopy (SEM, Jeol JSM 6400 model, Japan). Furthermore, atomic force microscopy (AFM, Nanosurf AG FlexAFM model with a 10 μm high resolution scan head, Switzerland) and fluorescence microscopy (Olympus BX53F, equipped with a CCD camera (Olympus DP72)) were also used for the surface imaging after deposition of the biofilm on transparent indium tin oxide (ITO) glasses by spin-coating technique.

Electrochemical Measurements. Electrochemical measurements of the PT-NH_2-g-PEG/Lac responses were carried out chronoamperometrically in working buffer solution by applying a potential of −0.05 V. A three-electrode system consisted of the GE as the working electrode, platinum as the counter electrode and Ag/AgCl electrode as the reference electrode was used. Briefly, when the analyte is introduced into the reaction cell, immobilized Lac is oxidized by molecular oxygen and then, reduced again by phenolic substrates, acting as electron donors for the enzyme regeneration and then, the phenolic substrates are converted into quinone, phenoxy radicals, or both, and subsequently, these products can be reduced at the electrode surface.[30] All amperometric measurements were performed in a batch mode. The enzyme electrode was initially equilibrated in 10 mL of 50 mM sodium phosphate buffer (pH 6.5). Prior to the substrate addition, current signal was reached a steady-state value. Differences in the current responses after catechol injection into the reaction cell, were recorded as current signal (μA). Working buffer was refreshed and the electrodes were rinsed with distilled water after each trial. Each measurement was repeated at least three times. All reported data were calculated as the mean ± standard deviation (S.D).

Sample Application. Following the optimization and characterization steps, PT-NH_2-g-PEG/Lac biosensor was applied for the analysis of phenolic compounds in artificial wastewater sample with highly acidic and salty nature. The samples were injected instead of the substrate and recovery (%) was calculated using the standard curve for the phenol. Experimental analyses were performed in three replicates. Data were recorded as the mean ± SD. The measurements were carried out at ambient conditions (25 °C).

3. RESULTS AND DISCUSSION

Synthesis of Polythiophene with Primary Amine and PEG Side Groups (PT-NH_2-g-PEG). Discovery of the CPs paved the way for a new era in the field of organic materials. CPs, which present a number of considerable advantages consisting of biocompatibility, entrapment ability, controlled release of the biological molecules, ability to transfer charge from a biochemical reaction, are beneficial materials in drug delivery, tissue-engineering scaffolds and biosensors.[31,32] Even though it was synthesized several CPs to create a host structure for the biological studies, new pathways has to be developed for enhancing the specificity on cellular adhesion and improving biological sensing elements. By functionalizing the CPs, novel architectures on a basic CP backbone was successfully accomplished to use in biomedical engineering and biodetecting technologies.[33−35] Among these type of functionalized CPs, graft copolymers that were generated with well-defined PEG chains are in attention, recently and provide more biocompatible and increased hydrophilicity.[36−38] In this concept, a graft copolymer was synthesized by incorporating PEG and -NH_2 moieties to the main-chain PT structure. In related works from the authors' laboratory, it was previously reported that PTs can be combined with various synthetic polymers by the electropolymerization of the corresponding thiophene macromonomers.[39−42] The strategy for obtaining the designed novel architecture referred as "PT-NH_2-g-PEG" pertains to the independent synthesis of the Suzuki coupling components. First, water-soluble thiophene macromonomer with PEG chain was prepared by taking advantages of Steglich esterification which is well-known method under mild conditions with the favorable catalytic action of 4-dimethylaminopyridine (DMAP).[11] The macromonomer, DBT-PEG was readily synthesized by a two-step procedure: (1) *N*-bromosuccinimide (NBS) bromination of thiophene-3-carboxylic acid and (2) esterification reaction of 2,5-dibrominated 3-thiophene carbox-

DOI: 10.1021/acsami.5b04967
ACS Appl. Mater. Interfaces 2015, 7, 20612−20622

ylic acid (**1**) with commercially available poly(ethylene glycol) monomethyl ether (Scheme 1).[43]

Scheme 1. Synthesis of Dibromothiophene-Functional PEG Macromonomers, DBT-PEG

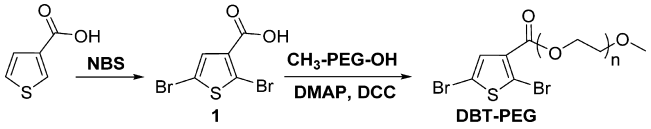

To pave the way of amino functional conducting polymers with water-soluble sequences as effective candidates for biological applications, the other component, 2,5-dibromothiophen-3-yl)methanamine (MA-DBT) was prepared via Gabriel sysnthesis[44] through transformation of primary alkyl halides into primary amines. The synthetic work presented in Scheme 2 involves two different bromination techniques of thiophen-3-

Scheme 2. Synthesis of Primary Amine Functional Monomer, MA-DBT

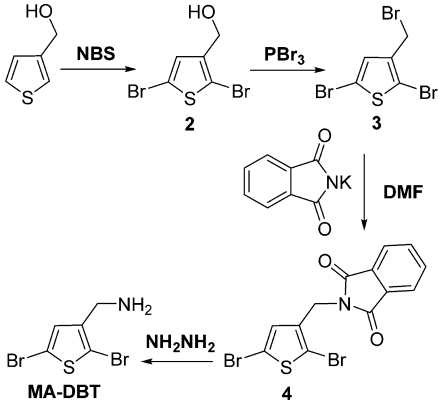

ylmethanol to reach the intermediate **3**. Then, the substitution reaction with the conjugate base of phthalimide gave the corresponding *N*-alkyl phthalimide, 2-((2,5-dibromothiophen-3-yl)methyl)isoindoline-1,3-dione (**4**). The yield of reaction was considerably increased by using preformed potassium salt of phthalimide, instead of phthalimide, facilitating the reaction to be conducted in a polar protic solvent such as DMF under homogeneous conditions. Reaction of the imide derivative, **4**, with hydrazine in the presence of methanol results in the formation of the final primary amine, MA-DBT. Phthalhydrazide formed as a byproduct was readily eliminated due to the low solubility in organic solvents.

Experimentally, PT-NH_2-*g*-PEG was synthesized by Suzuki polycondensation of the DBT-PEG macromonomer and MA-DBT in combination with 2,5-thiophenediboronic acid. Polymerization was carried out in homogeneous suspension of THF/water with potassium carbonate in the presence of palladium catalyst (Scheme 3). The reaction time was deliberately prolonged to 4 days so as to overcome steric limitations of the macromonomers and obtain graft copolymers with adequate molecular weight. Molecular weight characteristics of the starting macromonomer and the final polymer are given in Table 1. Expectedly, the graft copolymer has much higher molecular weight compare to that of the macromonomer. The broader molecular weight distribution of the

Scheme 3. Synthesis of Polythiophene with Primary Amine and PEG Side Groups (PT-NH_2-*g*-PEG)

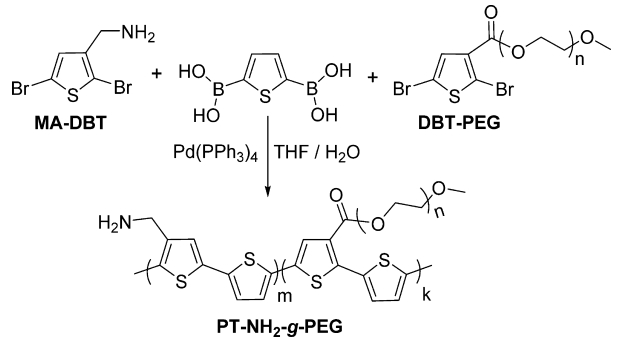

Table 1. Molecular Weight Characteristics of the Starting Macromonomer and Graft Copolymer

polymer	M_n (g mol^{-1})[a]	M_w/M_n[a]
DBT-PEG	5500	1.24
PT-NH_2-*g*-PEG	9100	2.06

[a]Determined by GPC with light scattering detector according to polystyrene standards.

graft copolymer may be attributed to the nature of the step-growth polymerization.

The structure of PT-NH_2-*g*-PEG was confirmed by ^{1}H NMR analysis. As can be seen Figure 1, in addition to characteristic

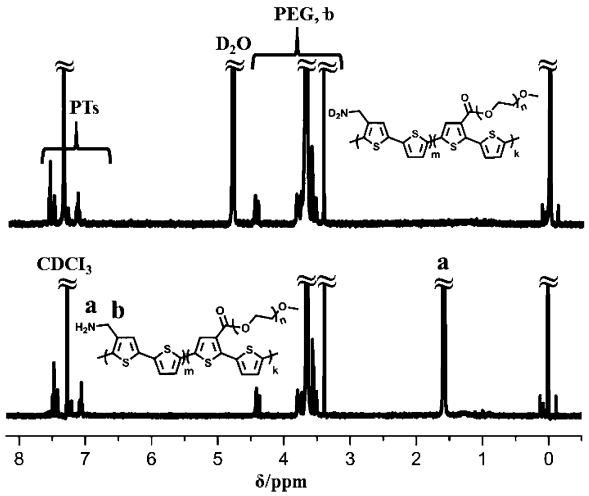

Figure 1. ^{1}H NMR spectra of PT-NH_2-*g*-PEG (a) before and (b) after proton exchange.

signals of PEG and PTs units, the primary amine protons appear at 1.58 ppm. Notably, these protons disappear after D_2O proton exchange clearly verifying the presence of primary amine groups in the structure.

Photophysical properties of the graft copolymer were also investigated in dilute DMF solution. As can be seen from Figure S7 (Supporting Information) where UV−vis absorption spectra of PT-NH_2-*g*-PEG and its precursors were recorded, the final graft copolymer exhibits strong broad absorption band at 300−425 nm arising from the supplementary conjugated thiophene rings in the main chain.

Figure S8 (Supporting Information) shows the fluorescence spectra of PPP-NH_2-*g*-PEG with a nearly mirror-image relation

DOI: 10.1021/acsami.5b04967
ACS Appl. Mater. Interfaces 2015, 7, 20612−20622

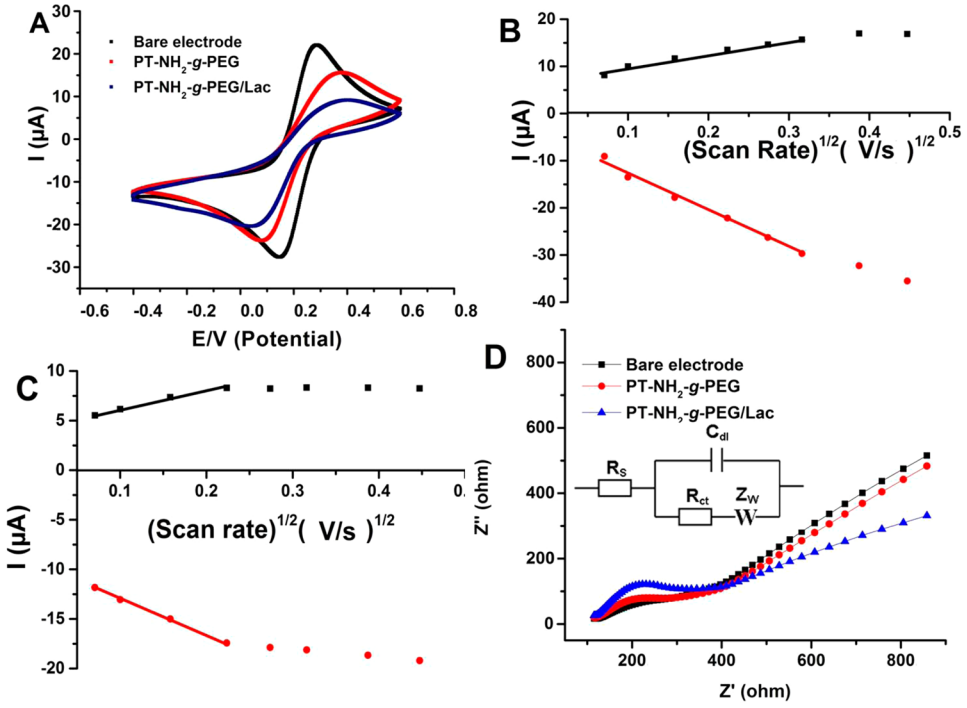

Figure 2. (A) Cyclic voltammograms of modified surfaces on graphite electrodes. (B and C) Scan rate effect of PT-NH_2-*g*-PEG coated and PT-NH_2-*g*-PEG/Lac coated surfaces. (D) Nyquist diagrams of modified surfaces on graphite electrodes. [Measurements were carried out in 50 mM sodium phosphate buffer (pH 6.5) in the presence of 5.0 mM $[Fe(CN)_6]^{3-/4-}$ and 0.1 M KCl].

between absorption and emission spectra. It is also seen that while the excitations in both solvents present similar trend, the corresponding emission in water is slightly blue-shifted relative to that in DMF. Table S1 (Supporting Information) summarizes photophysical data of the studied polymer in the dilute DMF and water solution. The absorption and emission of the graft polymer are essentially determined by the basic chromophore system of coumarin 1 solution according to the IUPAC technical report.[45]

It should also be noted that the fluorescence spectrum has a small shoulder emission at lower wavelength which may arise from the random placement of the macromonomer sequences in the backbone. Moreover, the aggregations that are taking place during the nanoparticles formation through the self-assembling of PTs backbones in solution create the blue-shifted shoulders in asymmetric shape.[46,47] In fact, this aggregation derives from strong interactions between hydrophobic backbones and aromatic $\pi-\pi$ stacking of conjugated backbone in water that severely decreases their water solubility and photoluminescent quantum efficiency.[48−50]

Preparation and Surface Characterization of PT-NH_2-*g*-PEG/Lac Biosensor. Biosensor was prepared by the immobilization of enzyme Lac onto PT-NH_2-*g*-PEG. The amine groups present in the structure of the graft copolymer enables cross-linking of the enzyme with the aid of GA. PT-NH_2-*g*-PEG/Lac biofilm covered on graphite electrode was characterized using both electrochemical and microscopic techniques. As the electrochemical techniques, CV and EIS measurements were performed to detect the electrochemical behavior on GEs. CVs for bare electrode, PT-NH_2-*g*-PEG and PT-NH_2-*g*-PEG/Lac surfaces were compared via current responses in the CV diagrams (Figure 2A). The decrease in the anodic and cathodic current peaks was monitored step-by-step. The oxidation and reduction peak potentials are obtained as 0.28 and 0.14 V for bare electrode (peak-to-peak separation of 0.14 V), 0.38 and 0.08 V for PT-NH_2-*g*-PEG modified electrode (peak-to-peak separation of 0.3 V) and 0.4 and 0.04 V for PT-NH_2-*g*-PEG/Lac electrodes (peak-to-peak separation of 0.36 V). The observed values indicate that the electron transfer between electrode and electrolytes were hindered due to the presence of the coating on the surface, demonstrating successful immobilization of Lac and polymer on GE. In a previous study, a similar behavior was observed when GE was coated with poly(BODT-*co*-FMOC) conducting copolymer film to monitor the inhibition effect of drugs on immobilized acetylcholinesterase/choline oxidase. Likewise, the peak potentials was shifted and decreased after coating the electrode.[51] It is quite reasonable that randomly adsorbed polymer on the electrode could affect the peak currents after the modification due to the PEG groups on the backbone of PT. PEG residues could also interact with the graphite and impede the contact of water-soluble redox probe with the surface. Additionally, a diffusion problem due to the presence of both biomolecule and polymer cross-linked on the surface, may also contribute to the observed drop. On the other hand, to monitor the electrocatalytic property of the polymer, a broad potential range between −0.4 and 1.4 V was applied to PT-NH_2-*g*-PEG coated and bare electrodes in 50 mM pH 6.5 phosphate buffer without using the redox mediator. As depicted in Figure S9 (Supporting Information), the peak currents belong to the PT-NH_2-*g*-PEG significantly increased compare to the bare graphite due to the presence of PT structure indicating successful covering of the surface with the conducting polymer.

To understand the diffusion phenomena on modified surfaces, we investigated anodic and cathodic current peaks belong to PT-NH_2-*g*-PEG and PT-NH_2-*g*-PEG/Lac according to electrochemical mechanisms at various scan rates (5.0−200

DOI: 10.1021/acsami.5b04967
ACS Appl. Mater. Interfaces 2015, 7, 20612−20622

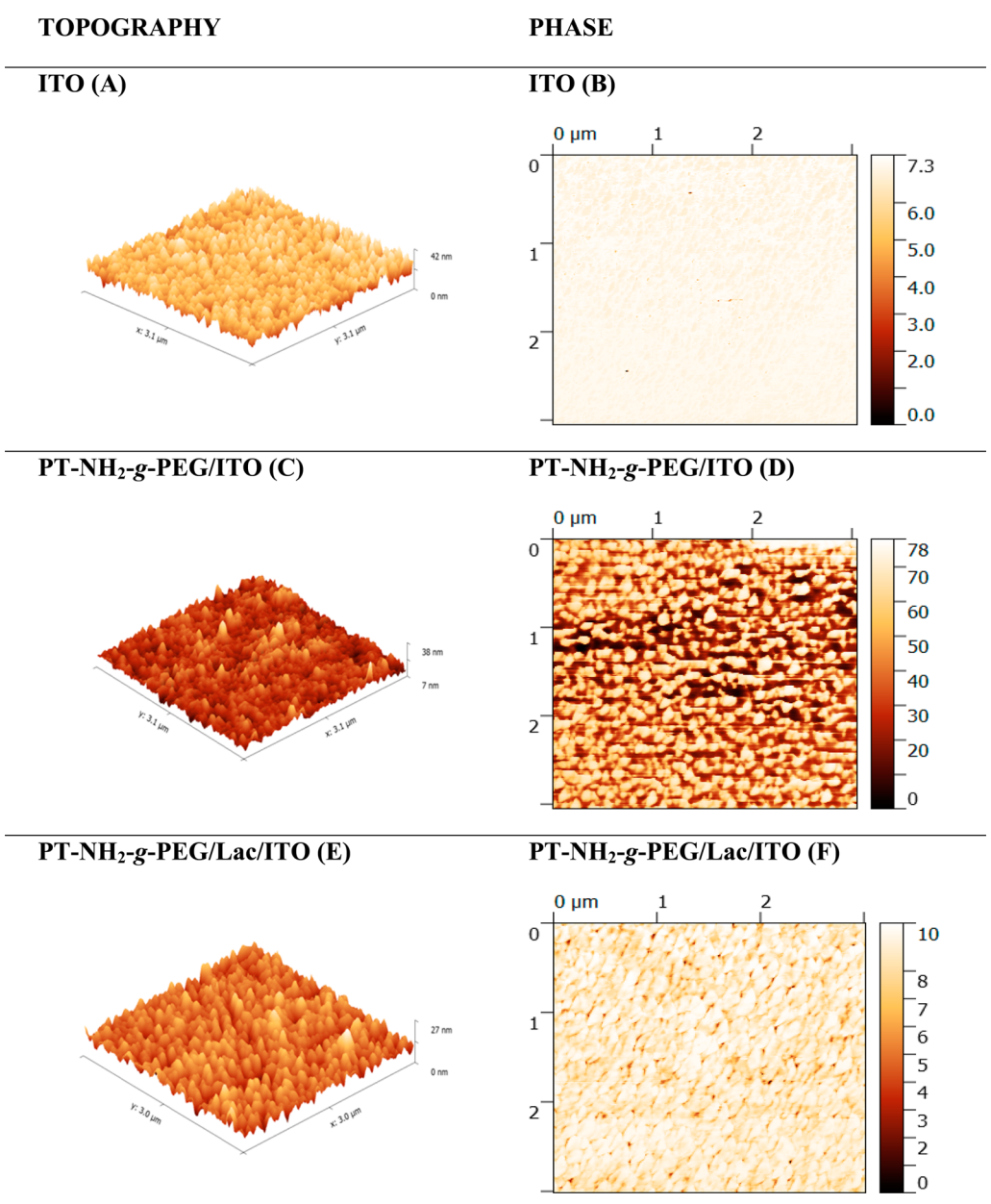

Figure 3. AFM 3D and phase histograms of the plain ITO, PT-NH_2-*g*-PEG/ITO, and PT-NH_2-*g*-PEG/Lac/ITO surfaces.

mV/s) in the presence of $[Fe(CN)_6]^{3-/4-}$ containing 0.1 M KCl solution. According to the results presented in Figure 2B,C, polymer coated and polymer-enzyme coated surfaces created a semilinear diffusion controlled electron transfer in a manner similar to that of the physical adsorption of intercalated montmorillonite and microbial cells.[17] The linear equations obtained from the scan rate effect were defined by the following equations; for PT-NH_2-*g*-PEG anodic and cathodic linear equations are $y = 26.2x + 7.5$ ($R^2 = 0.997$) and $y = 74.28x - 5.97$ ($R^2 = 0.998$), for PT-NH_2-*g*-PEG/Lac anodic and cathodic linear equations are $y = 18.17x + 4.32$ ($R^2 = 0.991$). At higher scan rates, the current peaks deviated from linearity. The linearity designates that the magnitude of the current is dominated by the diffusive mass transport, although the deviation at high scan rate indicates that insufficient solute reaches to the electrode surface. The exponential peak currents were monitored at the higher scan rate from 100 mV/s for PT-NH_2-*g*-PEG film and 75 mV/s for PT-NH_2-*g*-PEG/Lac film. The peak potentials were also found to be dependent on the scan rate indicating a quasireversible character of the electrode process. Beside these, a further study with CV technique was conducted to calculate the thickness of the polymer modified electrode by scanning the electrode between −0.4 and 1.4 V at 100 mV/s. The thickness of the PT-NH_2-*g*-PEG film formed by physical adsorption was found as 3.0 nm (equivalent of a 0.135 mC charge).

EIS analysis also gives idea about the surface modification processes. In this study, after the detailed CV interpreting, EIS measurements were carried out to prove the modification of polymer-enzyme biofilm. In a Nyquist plot, the semicircular corresponds to the electron-transfer resistance at the higher frequency range, which controls the electron transfer kinetics of the redox probe on the electrode−electrolyte solution interface. The diameter of the semicircle defines resistance of electron transfer. In general, the spectra consist of both the semicircular and linear parts. The obtained spectra can be modeled with

DOI: 10.1021/acsami.5b04967
ACS Appl. Mater. Interfaces 2015, 7, 20612−20622

equivalent circuit models, which are helpful for interpreting the electrical properties of the surface of the biosensor. As shown in the Figure 2D, the EIS spectra from the modified surfaces contain both a semicircle and a linear part. Randle's equivalent circuit model was applied to fit results. The circuit model includes the solution resistance (R_s), the Warburg impedance (Z_w) resulting from the diffusion of the $[Fe(CN)_6]^{3-/4-}$ redox probe, the double layer capacitance (C_{dl}) and the charge transfer resistance (R_{ct}).[52,53] The properties of the electrode interface are defined by R_{ct} which is highly sensitive to the surface structure. According to the semicircle diameters, there was a dramatic increase due to the modification of electrode. The corresponding R_{ct} values are 249 Ω for bare graphite, 321 Ω for PT-NH_2-*g*-PEG and 493 Ω for PT-NH_2-*g*-PEG/Lac film. This issue can be explained by the modification of the film. Moreover, it can be seen that the findings from CV results are in accordance with EIS results.

In addition to the electron transfer properties of PT-NH_2-*g*-PEG/Lac surface, microscopic techniques such as AFM, fluorescence microscopy, and SEM investigations were carried out to illustrate the differences between modified surfaces using transparent ITO electrodes. AFM is the one of the most adopted method for the characterization of polymers, since nonconductive materials can also be analyzed. Moreover, its sample preparation procedure is easier and it gives more useful information than SEM and transmission electron microscopy analyses.[54] In the Figure 3A,B, the basic information about classic ITO topographic surface and also phase histograms are presented. Topography map bestows morphological data such as roughness and phase diagram. Accordingly, it can be understood from the phase differences between the samples, whether the studied surfaces was uniformly coated or not.[55] 3D Topographical maps show that plain ITO have more homogeneous pattern than PT-NH_2-*g*-PEG coated on ITO. Moreover, Lac immobilized PT-NH_2-*g*-PEG/ITO surface also generated a uniform layer (Figure 3A,C,E). Apart from this, the roughness data of the samples illustrates the difference between modified surfaces as plain ITO, PT-NH_2-*g*-PEG/ITO, and PT-NH_2-*g*-PEG//Lac/ITO have the values of 3.61, 2.31, and 2.06 nm, respectively. Phase histograms gives more information than topographic map as the amount of details contained is limited by the surface roughness.[56] According to our study, ITO surface have homogeneous rough area and showed one phase on the phase histogram. On the other hand, polymer coating changes the surface roughness and both polymer and ITO phases could be seen in the phase histograms at the same time. Additionally, as illustrated in phase histograms (Figure 3B,D,F), enzyme coating caused a significant decrease in roughness.

Besides AFM analysis, fluorescence images were taken to confirm PT-NH_2-*g*-PEG deposition and enzyme covering. The self-fluorescence properties of the polymer enables to visualize the modified surface and immobilized enzymes can clearly be seen as spots under the fluorescence microscope (Figure 4).

As a final surface characterization optimized biofilm layer was monitored via SEM technique. The general morphology of the PT-NH_2-*g*-PEG/Lac on graphite rod was evidently shown in Figure S10 (Supporting Information). The figure suggests that the surface of graphite is completely covered by the polymer and enzymes could be covalently linked through the cross-linking reaction of GA favored by the porous structure resulted from the presence of hydrophilic PEG segments.

Optimization and Analytical Characterization. The pH change in the environment of biologically active structures like

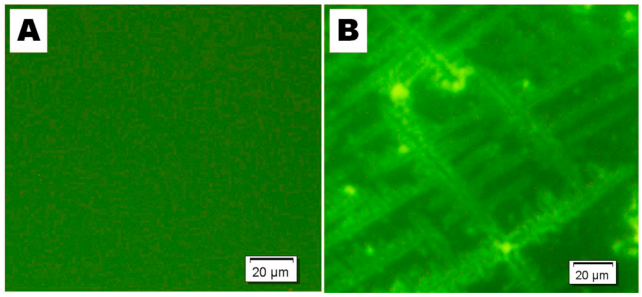

Figure 4. (A) PT-NH_2-*g*-PEG and (B) PT-NH_2-*g*-PEG/Lac surfaces on ITO glass.

enzymes affects their three-dimensional structure and charge. Accordingly, the success of the enzymatic catalysis process strongly depends on the pH conditions. Therefore, defining optimum pH values for the enzyme electrode is one of the important parameters. Biosensor response was recorded at various pH values using phosphate buffer systems in the range of 5.5−7.5 using 0.0125 mM catechol as phenolic substrate. Higher peak current was obtained at pH 6.5 (Figure 5).

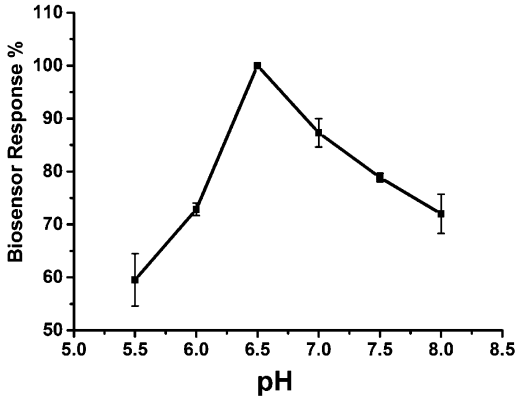

Figure 5. Effect of pH on the responses of PT-NH_2-*g*-PEG/Lac biosensor. Measurements were carried out at −0.05 V vs Ag/AgCl and 50 mM sodium phoshate buffer in the presence of 0.0125 mM catechol under ambient conditions. Error bars show the standard deviation (±SD) of three measurements.

Generally, the maximum activity of Lac immobilized on solid supports was observed between 5.0 and 6.0.[57,58] Further biosensing applications were carried out at pH 6.5 phosphate buffer solution.

The effect of polymer amount used in biosensor construction was also examined. Following the preparation of biofilm layers by using different amounts of the polymer, calibration curves were generated with the addition of catechol standard solutions. Figure 6A demonstrates the general behavior of the PT-NH_2-*g*-PEG/Lac biofilms prepared in different amounts. The biosensor constructed with 0.25 and 1.0 mg PT-NH_2-*g*-PEG gave a similar linear equation. For 0.25 mg PT-NH_2-*g*-PEG, the linear range is between 0.0075−0.1 mM defined by the equation of $y = 14.43x - 0.023$ ($R^2 = 0.997$). When 1.0 mg polymer was used, the linearity was in the range of 0.01−0.5 mM and defined by the equation of $y = 13.19x - 0.099$, ($R^2 = 0.998$). Apparently, the biosensor constructed with 0.5 mg PT-NH_2-*g*-PEG showed the highest higher current responses in compared to the others. The detection range was 0.0025−0.05 mM ($y = 132.45x + 0.183$, ($R^2 = 0.998$)). In the case of

DOI: 10.1021/acsami.5b04967
ACS Appl. Mater. Interfaces 2015, 7, 20612−20622

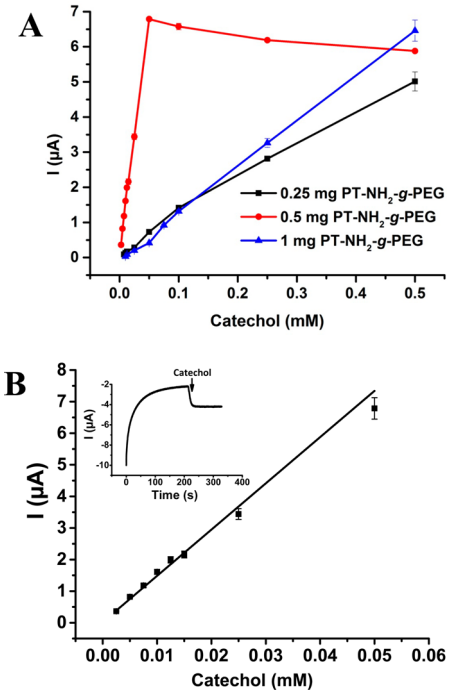

Figure 6. (A) Calibration curves belong to different polymer concentrations used in immobilization of Lac and (B) the calibration curve of PT-NH_2-*g*-PEG/Lac within the highest sensitivity. (B, Inset) Graph showing the 0.015 mM catechol addition. Measurements were carried out at −0.05 V vs Ag/AgCl and 50 mM sodium phoshate buffer in the presence of 0.0125 mM catechol under ambient conditions. Error bars show the standard deviation (±SD) of three measurements.

detection ranges for these calibration curves, 0.5 mg PT-NH_2-*g*-PEG exhibits better detection features with the concentration of 2.5 μM catechol (Figure 6B). Furthermore, greater sensitivity was obtained within this concept as 132.45 μA mM^{-1} when it was compared to other biosensors prepared with Lac (Table 2.) On the other hand, the response time for all constructed PT-NH_2-*g*-PEG/Lac biosensors were similar and less than 4 s.

The kinetic parameters of the constructed sensor which gave the best sensitivity were characterized using Lineveawer-Burk Diagrams.[59] The apparent Michaelis−Menten constant (K_m^{app}) and maximum current (I_{max}) were calculated as 0.026 mM and 7.38 μA, respectively. It is known that the low K_m^{app} value observed corresponds to a high enzyme affinity toward the substrate. In addition, the limit of detection (LOD) value of the PT-NH_2-*g*-PEG/Lac biosensor was calculated according to the equation $3S_b/m$, where S_b is the standard deviation of 10 measurements for the lowest concentration in the calibration curve, and m is the slope of the linear regression equation. It was found that the LOD of the proposed sensor system was 0.01 μM.

To investigate the interference effects on the biosensor response, several substrates such as uric acid, ascorbic acid, ethanol, and acetamidophenol (10 μM) were added to the reaction medium together with 12.5 μM catechol. The same catechol amount was also introduced into the reaction cell, and it was observed that initial and last catechol signals were similar. There was no dramatic change in the current responses when the 10 μM interferants were added into the reaction cell, as shown in Figure 7. As a result, constructive biosensor possessed good selectivity for the detection of phenolics in the presence of possible interfering compounds.

Other analytical parameters such as repeatability and operation stability, were also investigated. In a period of 12 days, operational performance of the PT-NH_2-*g*-PEG/Lac was investigated through 105 measurements, and it was found that the sensor retained 82% of its initial activity. It should be pointed out that the optimized biosensor was kept at 4 °C when not in use and standard deviation (±SD) and coefficient of variation were found to be 0.05 and 4.1%, respectively. All these results reveal that the described biosensor exhibits higher accuracy and stability compare to the systems prepared by physical adsorption. Besides the operational stability, repeatability was tested upon 10 successive measurements in the same day.

Table 2. Comparison of the Various Laccase Biosensors for the Detection of Phenolic Compounds

modified electrode	immobilization method	linear range (mM)	sensitivity (μA/mM)	K_m^{app} (mM)	I_{max} (μA)	op. stability	ref
AuNP/Fullerenols/SPE	covalent immobilization (SAM)	0.03−0.3	ND	0.66	6.00	87% in 120 days	60
SiO_2−PA NPs/GCE	adsorption	0.0009−0.103	ND	ND	ND	80% in 40 days	61
ERM/Pt	entrapment/cross-linking	0.0005−0.05	ND	0.0387	0,31	60% in 10 months	19
modified graphite/CPE	entrapment	0.197−3.24	ND	3.87	ND	ND	62
nafion/BP2000/GCE	entrapment	0.003−0.005	99.84	1.79	51.282	96.1% in 20 days	63
polyethersulphone membranes/Pt electrode	entrapment	0.002−0.014	0.0566	ND	ND	ND	64
mesoporous silica/GCE	encapsulation	0.002−0.1	2.63	ND	ND	100% in 50 days	65
polyethersulphone membranes/Pt	covalent immobilization	0.01−0.110	0,0216	ND	ND	38% in 38 days	66
HMDA/Graphite electrode	covalent immobilization	Up to 0.1	196	0,18	45	No decrease in 30 days	67
MB-MCM-41/PVA/Au electrode	entrapment	0.004−0.088	ND	0.256	69.589	ND	68
PT-NH_2-*g*-PEG/GE	adsorption	0.0025−0.5	132.45	0.026	7.38	82.08% in 12 days	this work

Op. stability, operational stability; AuNP, gold nanoparticle; SPE, screen printed electrode; SAM, self-assembled monolayer; SiO_2−PA NPs, phtyic acid coated silica nanoparticles; GCE, glassy carbon electrode; ERM, epoxy resin membrane; Pt, platinum electrode; CPE, carbon paste electrode; B2000, Black Pearl 2000 electrochemical catalyst; PVA, poly(vinyl alcohol); MB, methylene blue; MCM-41, mesoporous silica sieve; ND, not detected.

DOI: 10.1021/acsami.5b04967
ACS Appl. Mater. Interfaces 2015, 7, 20612−20622

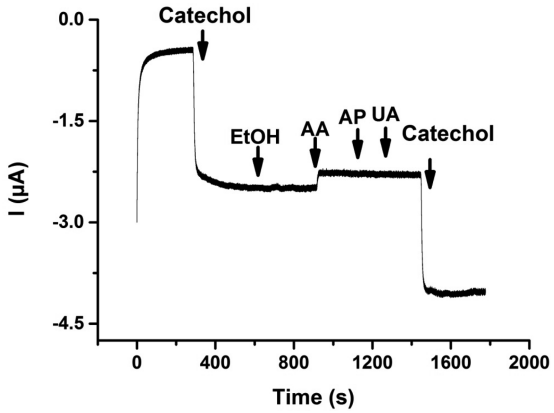

Figure 7. Effect of some substrates (10 μM) added into the cell on the sensor response measured at −50 mV in pH 6.5 phosphate buffer. Catechol was added to be 15 μM in the cell for comparison; (EtOH) ethanol, (AA) ascorbic acid, (AP) 3-acetamidophenol, and (UA) uric acid.

Sample Application. In the final part of the work, the developed biosensor was applied to detect phenol in artificial wastewater which was prepared using 1.0 M HCl solution containing 50 g/L NaCl and 100 g/L phenol. Prior to sample application, a new calibration curve for phenol was produced with the equation of $y = 19.1x + 0.063$, ($R^2 = 0.993$) and at the detection range of 0.005−0.1 mM phenol. Following the definition of phenol linearity characteristics, artificial wastewater was diluted 10 times in the working buffer, and the final solution was added into the reaction cell for the application. The corresponding results were compared with those obtained using known concentrations and 101.8% recovery ($n = 4$) was achieved. These results indicate the graft copolymer immobilized with Lac is an efficient biosensor for the detection phenolic compounds.

4. CONCLUSION

A functional conducting polymer decorated with the PEG groups was synthesized by Suzuki coupling process in several steps, and the obtained amino functionalized matrix was successfully conducted to biosensing applications for the analysis of phenolic compounds. In the synthetic strategy, PEG and amine functional dibromothiophenes were prepared independently and subsequently used in Suzuki polycondensation in conjunction with 2,5-thiophenediboronic acid using palladium catalyst to yield the desired graft copolymer. The data obtained from intense surface characterization suggest that the hybrid graft PT-NH_2-*g*-PEG copolymer immobilized with Lac was successfully coated on the surface of the electrode by generating a homogeneous thin film. Kinetic parameters (sensitivity, K_m^{app}, I_{max}) of the proposed biofilm bearing biocompatible PEG residues demonstrate the enhanced biosensor performance with the retaining activity of enzyme compare to the other reported works (Table 2). The distinct advantages of the biosensor also include a good recovery and applicability to real samples as demonstrated with artificial wastewater test. Inspired by the successful immobilization of Lac enzyme and subsequent application as biosensor for the determination of phenolic compounds, further studies are being carried out in our laboratories focusing on the use of other enzymes and their corresponding biosensor applications.

■ ASSOCIATED CONTENT

Supporting Information

The Supporting Information is available free of charge on the ACS Publications website at DOI: 10.1021/acsami.5b04967.

^{1}H NMR of spectra of the compounds, 1, 2, 3, 4, and DBT-PEG and MA-DBT; photophysical properties of polymer; cyclic voltammograms of PT-NH_2-*g*-PEG film; SEM image of PT-NH_2-*g*-PEG/Lac biofilm. (PDF)

■ AUTHOR INFORMATION

Corresponding Authors

*E-mail: sunatimur@yahoo.com. suna.timur@ege.edu.tr. Tel.: +90 2323115487. Fax: +90 2323115485.

*E-mail: yusuf@itu.edu.tr.

Notes

The authors declare no competing financial interest.

■ ACKNOWLEDGMENTS

Dr. Mustafa Can and F. B. Barlas are gratefully acknowledged for their support in AFM measurements. This study has no further funding sources.

■ ABBREVIATIONS

CP	conducting polymer
PT	polythiophene
Lac	laccase
CNT	multiwalled carbon nanotube
PPy	polypyrrole
PT-NH_2-*g*-PEG	polythiophene-NH_2-*g*-polyethylene glycol
GE	graphite electrode
GA	glutaraldehyde
THF	tetrahydrofuran
CV	cyclic voltammetry
EIS	electrochemical impedance spectroscopy
SEM	scanning electron microscopy
AFM	atomic force microscopy
ITO	indium tin oxide
AuNP	gold nanoparticle
SPE	screen printed electrode
SAM	self-assembled monolayer
SiO_2−PA NPs	phtyic acid coated silica nanoparticles
GCE	glassy carbon electrode
ERM	epoxy resin membrane
Pt	platinum electrode
CPE	carbon paste electrode
B2000	Black Pearl 2000 electrochemical catalyst
PVA	poly(vinyl alcohol)
MB	methylene blue
MCM-41	mesoporous silica sieve
ND	not detected

■ REFERENCES

(1) Hollister, S. J. Porous Scaffold Design for Tissue Engineering. *Nat. Mater.* **2005**, *4*, 518−524.

(2) Langer, R.; Tirrell, D. A. Designing Materials for Biology and Medicine. *Nature* **2004**, *428*, 487−492.

(3) MacDiarmid, A. G. Synthetic Metals: A Novel Role for Organic Polymers (Nobel Lecture). *Curr. Appl. Phys.* **2001**, *1*, 269−279.

(4) Janata, J.; Josowicz, M. Conducting Polymers in Electronic Chemical Sensors. *Nat. Mater.* **2003**, *2*, 19−24.

(5) Akbulut, H.; Yavuz, M.; Guler, E.; Odaci Demirkol, D.; Yamada, S.; Endo, T.; Timur, S.; Yagci, Y. Electrochemical Deposition of

DOI: 10.1021/acsami.5b04967
ACS Appl. Mater. Interfaces 2015, 7, 20612−20622

Polypeptides: Bio-based Covering Materials for Surface Design. *Polym. Chem.* **2014**, *5*, 3929−3936.
(6) Demirci Uzun, S.; Kayaci, F.; Uyar, T.; Timur, S.; Toppare, L. Bioactive Surface Design based on Functional Composite Electrospun Nanofibers for Biomolecule Immobilization And Biosensor Applications. *ACS Appl. Mater. Interfaces* **2014**, *6*, 5235−5243.
(7) Albers, W. M.; Pelto, J. M.; Suspene, C.; Maättä, J. A.; Yassar, A.; Hytönen, V. P.; Vikholm-Lundin, I. M.; Tappura, K. Structural and Functional Characteristics of Chimeric Avidins Physically Adsorbed onto Functionalized Polythiophene Thin Films. *ACS Appl. Mater. Interfaces* **2012**, *4*, 4067−4077.
(8) Kesik, M.; Akbulut, H.; Soylemez, S.; Cevher, S. C.; Hizalan, G.; Udum, Y. A.; Endo, T.; Yamada, S.; Cirpan, A.; Yagci, Y.; Toppare, L. Synthesis and Characterization of Conducting Polymers Containing Polypeptide and Ferrocene Side Chains as Ethanol Biosensors. *Polym. Chem.* **2014**, *5* (21), 6295−6306.
(9) Akbulut, H.; Endo, T.; Yamada, S.; Yagci, Y. Synthesis and Characterization of Polyphenylenes with Polypeptide and Poly(ethylene glycol) Side Chains. *J. Polym. Sci., Part A: Polym. Chem.* **2015**, *53*, 1785.
(10) Ahuja, T.; Mir, I. A.; Kumar, D.; Rajesh. Biomolecular Immobilization on Conducting Polymers for Biosensing Applications. *Biomaterials* **2007**, *28*, 791−805.
(11) Colak, D. G.; Cianga, I.; Demirkol, D. O.; Kozgus, O.; Medine, E. I.; Sakarya, S.; Unak, P.; Timur, S.; Yagci, Y. The Synthesis and Targeting of PPP-type Copolymers to Breast Cancer Cells: Multifunctional Platforms for Imaging and Diagnosis. *J. Mater. Chem.* **2012**, *22* (18), 9293−9300.
(12) Jenekhe, S. A. A Class of Narrow-Band-Gap Semiconducting Polymers. *Nature* **1986**, *322* (6077), 345−347.
(13) Yao, Z.; Hu, X.; Huang, B.; Zhang, L.; Liu, L.; Zhao, Y.; Wu, H.-C. Halochromism of a Polythiophene Derivative Induced by Conformational Changes and Its Sensing Application of Carbon Dioxide. *ACS Appl. Mater. Interfaces* **2013**, *5* (12), 5783−5787.
(14) Toy, P. H.; Janda, K. D. Soluble Polymer-Supported Organic Synthesis. *Acc. Chem. Res.* **2000**, *33* (8), 546−554.
(15) Reuss, V. S.; Obermeier, B.; Dingels, C.; Frey, H. N,N-Diallylglycidylamine: A Key Monomer for Amino-Functional Poly(ethylene glycol) Architectures. *Macromolecules* **2012**, *45* (11), 4581−4589.
(16) Glezer, V. Environmental Effects of Substituted Phenols. In *The Chemistry of Phenols*. Rappoport, Z., Ed.; John Wiley & Sons, Ltd.: West Sussex, U.K., 2003, Vol.2, 1347−1368.
(17) Karim, F.; Fakhruddin, A. N. M. Recent Advances in the Development of Biosensor for Phenol: A Review. *Rev. Environ. Sci. Bio/Technol.* **2012**, *11* (3), 261−274.
(18) Borgmann, S.; Schulte, A.; Neugebauer, S.; Schuhmann, W. Amperometric Biosensors. *Adv. Electrochem. Sci. Eng.* **2012**, *13*, 1−83.
(19) Chawla, S.; Rawal, R.; Shabnam; Kuhad, R. C.; Pundir, C. S. An Amperometric Polyphenol Biosensor based on Laccase Immobilized on Epoxy Resin Membrane. *Anal. Methods* **2011**, *3*, 709−714.
(20) Oliveira, T. M. B. F.; Barroso, M. F.; Morais, S.; de Lima-Neto, P.; Correia, A. N.; Oliveira, M. B. P. P.; Delerue-Matos, C. Biosensor Based on Multi-Walled Carbon Nanotubes Paste Electrode Modified with Laccase for Pirimicarb Pesticide Quantification. *Talanta* **2013**, *106*, 137−143.
(21) Diaconu, M.; Litescu, S. C.; Radu, G. L. Bienzymatic Sensor Based on the Use of Redox Enzymes and Chitosan−MWCNT Nanocomposite. Evaluation of Total Phenolic Content in Plant Extracts. *Microchim. Acta* **2011**, *172*, 177−184.
(22) Gutiérrez-Sánchez, C.; Jia, W.; Beyl, Y.; Pita, M.; Schuhmann, W.; De Lacey, A. L.; Stoica, L. Enhanced Direct Electron Transfer Between Laccase and Hierarchical Carbon Microfibers/Carbon Nanotubes Composite Electrodes. Comparison of Three Enzyme Immobilization Methods. *Electrochim. Acta* **2012**, *82*, 218−223.
(23) Ibarra-Escutia, P.; Juarez-Gómez, J.; Calas-Blanchard, C.; Marty, J. L.; Ramírez-Silva, M. T. Amperometric Biosensor Based on a High Resolution Photopolymer Deposited onto a Screen-Printed Electrode for Phenolic Compounds Monitoring in Tea Infusions. *Talanta* **2010**, *81*, 1636−1642.
(24) Montereali, M. R.; Seta, L. D.; Vastarella, W.; Pilloton, R. A Disposable Laccase−Tyrosinase Based Biosensor for Amperometric Detection of Phenolic Compounds in Must and Wine. *J. Mol. Catal. B: Enzym.* **2010**, *64*, 189−194.
(25) Vianello, F.; Cambria, A.; Ragusa, S.; Cambria, M. T.; Zennaro, L.; Rigo, A. A High Sensitivity Amperometric Biosensor Using a Monomolecular Layer of Laccase as Biorecognition Element. *Biosens. Bioelectron.* **2004**, *20*, 315−321.
(26) Wang, Z.; Xu, Q.; Wang, J. H.; Yang, Q.; Yu, J. H.; Zhao, Y. D. Ascorbic Acid Biosensor Based on Laccase Immobilized on an Electrode Modified with a Self-Assembled Monolayer and Coated with Functionalized Quantum Dots. *Microchim. Acta* **2009**, *165*, 387−392.
(27) Brondani, D.; De Souza, B.; Souza, B. S.; Neves, A.; Vieira, I. C. PEI-Coated Gold Nanoparticles Decorated with Laccase: A New Platform for Direct Electrochemistry of Enzymes and Biosensing Applications. *Biosens. Bioelectron.* **2013**, *42*, 242−247.
(28) Cesarino, I.; Galesco, H. V.; Moraes, F. C.; Lanza, M. R. V.; Machado, S. A. S. Biosensor Based on Electrocodeposition of Carbon Nanotubes/Polypyrrole/Laccase for Neurotransmitter Detection. *Electroanalysis* **2013**, *25*, 394−400.
(29) Songurtekin, D.; Yalcinkaya, E. E.; Ag, D.; Seleci, M.; Odaci Demirkol, D.; Timur, S. Histidine Modified Montmorillonite: Laccase Immobilization and Application to Flow Injection Analysis of Phenols. *Appl. Clay Sci.* **2013**, *86*, 64−69.
(30) Haghighi, B.; Gorton, L.; Ruzgas, T.; Jönsson, L. J. Characterization of Graphite Electrodes Modified with Laccase from *Trametes versicolor* and Their Use for Bioelectrochemical Monitoring of Phenolic Compounds in Flow Injection Analysis. *Anal. Chim. Acta* **2003**, *487*, 3−14.
(31) Guimard, N. K.; Gomez, N.; Schmidt, C. E. Conducting Polymers in Biomedical Engineering. *Prog. Polym. Sci.* **2007**, *32*, 876−891.
(32) Bendrea, A. D.; Cianga, L.; Cianga, I. Review Paper: Progress in the Field of Conducting Polymers for Tissue Engineering Applications. *J. Biomater. Appl.* **2011**, *26*, 3−84.
(33) Li, D. F.; Wang, H. J.; Fu, J. X.; Wang, W.; Jia, X. S.; Wang, J. Y. Preparation of a Hydrophobic Polythiophene Film to Improve Protein Adsorption and Proliferation of PC 12 Cells. *J. Phys. Chem. B* **2008**, *112*, 16290−16299.
(34) Fabregat, G.; Ballano, G.; Armelin, E.; Del Valle, L. J.; Cativiela, C.; Aleman, C. An Electroactive and Biologically Responsive Hybrid Conjugate Based on Chemical Similarity. *Polym. Chem.* **2013**, *4*, 1412−1424.
(35) Perez-Madrigal, M. M.; Armelin, E.; Del Valle, L. J.; Estrany, F.; Aleman, C. Bioactive and Electroactive Response of Flexible Polythiophene:Polyester Nanomembranes for Tissue Engineering. *Polym. Chem.* **2012**, *3*, 979−991.
(36) Peyre, J.; Humblot, V.; Methivier, C.; Berjeaud, J.-M.; Pradier, C.-M. Co-Grafting of Amino−Poly(ethylene glycol) and Magainin I on a TiO_2 Surface: Tests of Antifouling and Antibacterial Activities. *J. Phys. Chem. B* **2012**, *116* (47), 13839−13847.
(37) Hamley, I. W.; Krysmann, M. J.; Castelletto, V.; Noirez, L. Multiple Lyotropic Polymorphism of a Poly(ethylene glycol)-Peptide Conjugate in Aqueous Solution. *Adv. Mater.* **2008**, *20*, 4394−4397.
(38) Xu, Y. Y.; Yuan, J. Y.; Fang, B.; Drechsler, M.; Mullner, M.; Bolisetty, S.; Ballauff, M.; Muller, A. H. E. Hybrids of Magnetic Nanoparticles with Double-Hydrophilic Core/Shell Cylindrical Polymer Brushes and Their Alignment in a Magnetic Field. *Adv. Funct. Mater.* **2010**, *20*, 4182−4189.
(39) Sahin, E.; Camurlu, P.; Toppare, L.; Mercore, V. M.; Cianga, I.; Yagci, Y. Synthesis and Characterization of Thiophene Functionalized Polystyrene Copolymers and Their Electrochemical Properties. *Polym. Int.* **2005**, *54* (12), 1599−1605.
(40) Sahin, E.; Camurlu, P.; Toppare, L.; Mercore, V. M.; Cianga, I.; Yagcı, Y. Conducting Copolymers of Thiophene Functionalized Polystyrenes with Thiophene. *J. Electroanal. Chem.* **2005**, *579* (2), 189−197.

DOI: 10.1021/acsami.5b04967
ACS Appl. Mater. Interfaces 2015, 7, 20612−20622

(41) Alkan, S.; Toppare, L.; Hepuzer, Y.; Yagci, Y. Synthesis and Characterization of Conducting Block Copolymers of Thiophene-Ended Polystyrene with Polypyrrole. *Synth. Met.* **2001**, *119* (1−3), 133−134.
(42) Alkan, S.; Toppare, L.; Hepuzer, Y.; Yagci, Y. Block Copolymers of Thiophene-Capped Poly(methyl methacrylate) with Pyrrole. *J. Polym. Sci., Part A: Polym. Chem.* **1999**, *37* (22), 4218−4225.
(43) McTiernan, C. D.; Chahma, M. H. Synthesis and Characterization of Alanine Functionalized Oligo/Polythiophenes. *New J. Chem.* **2010**, *34* (7), 1417−1423.
(44) Gibson, M. S.; Bradshaw, R. W. The Gabriel Synthesis of Primary Amines. *Angew. Chem., Int. Ed. Engl.* **1968**, *7* (12), 919−930.
(45) Brouwer, A. M. Standards for Photoluminescence Quantum Yield Measurements in Solution (IUPAC Technical Report). *Pure Appl. Chem.* **2011**, *83* (12), 2213−2228.
(46) Kim, H.-J.; Kim, T.; Lee, M. Responsive Nanostructures from Aqueous Assembly of Rigid-Flexible Block Molecules. *Acc. Chem. Res.* **2011**, *44* (1), 72−82.
(47) Pecher, J.; Mecking, S. Nanoparticles of Conjugated Polymers. *Chem. Rev.* **2010**, *110* (10), 6260−6279.
(48) Qin, C.; Wu, X.; Gao, B.; Tong, H.; Wang, L. Amino Acid-Functionalized Polyfluorene as a Water-Soluble Hg^{2+} Chemosensor with High Solubility and High Photoluminescence Quantum Yield. *Macromolecules* **2009**, *42* (15), 5427−5429.
(49) Feng, X.; Liu, L.; Wang, S.; Zhu, D. Water-Soluble Fluorescent Conjugated Polymers and Their Interactions with Biomacromolecules for Sensitive Biosensors. *Chem. Soc. Rev.* **2010**, *39* (7), 2411−2419.
(50) Zhu, B.; Han, Y.; Sun, M.; Bo, Z. Water-Soluble Dendronized Polyfluorenes with an Extremely High Quantum Yield in Water. *Macromolecules* **2007**, *40* (13), 4494−4500.
(51) Turan, J.; Kesik, M.; Soylemez, S.; Goker, S.; Kolb, M.; Bahadir, M.; Toppare, L. Development of an Amperometric Biosensor Based on a Novel Conducting Copolymer for Detection of Anti-dementia Drugs. *J. Electroanal. Chem.* **2014**, *735*, 43−50.
(52) Guo, X.; Kulkarni, A.; Doepke, A.; Halsall, H. B.; Iyer, S.; Heineman, W. R. Carbohydrate-Based Label-Free Detection of Escherichia coli ORN 178 Using Electrochemical Impedance Spectroscopy. *Anal. Chem.* **2012**, *84*, 241−246.
(53) Zhang, Z.; Wang, X.; Yang, X. A Sensitive Choline Biosensor Using Fe_3O_4 Magnetic Nanoparticles as Peroxidase Mimics. *Analyst* **2011**, *136*, 4960−4965.
(54) Kim, J. Y.; Lee, H. K.; Kim, S. C. Surface Structure and Phase Separation Mechanism of Polysulfone Membranes by Atomic Force Microscopy. *J. Membr. Sci.* **1999**, *163*, 159−166.
(55) Chapman, P.; Ducker, R. E.; Hurley, C. R.; Hobbs, J. K.; Leggett, G. J. Fabrication of Two-Component, Brush-On-Brush Topographical Microstructures by Combination of Atom-Transfer Radical Polymerization with Polymer End-Functionalization and Photopatterning. *Langmuir* **2015**, *31*, 5935−5944.
(56) Garcia, R.; Perez, R. Dynamic Atomic Force Microscopy Methods. *Surf. Sci. Rep.* **2002**, *47*, 197−301.
(57) Yaropolov, A. I.; Kharybin, A. N.; Emnéus, J.; Marko-Varga, G.; Gorton, L. Flow-Injection Analysis of Phenols at a Graphite Electrode Modified with Co-Immobilised Laccase and Tyrosinase. *Anal. Chim. Acta* **1995**, *308*, 137−144.
(58) Freire, R. S.; Thongngamdee, S.; Duran, N.; Wang, J.; Kubota, L. T. Mixed Enzyme (Laccase/Tyrosinase)-Based Remote Electrochemical Biosensor for Monitoring Phenolic Compounds. *Analyst* **2002**, *127*, 258−261.
(59) Lineweaver, L.; Burk, D. The Determination of Enzyme Dissociation Constants. *J. Am. Chem. Soc.* **1934**, *56*, 658−666.
(60) Lanzellotto, C.; Favero, G.; Antonelli, M. L.; Tortolini, C.; Cannistraro, S.; Coppari, E.; Mazzei, F. Nanostructured Enzymatic Biosensor Based on Fullerene and Gold Nanoparticles: Preparation, Characterization and Analytical Applications. *Biosens. Bioelectron.* **2014**, *55*, 430−437.
(61) Wang, K.; Liu, P.; Ye, Y.; Li, J.; Zhao, W.; Huang, X. Fabrication of a Novel Laccase Biosensor Based on Silica Nanoparticles Modified with Phytic Acid for Sensitive Detection of Dopamine. *Sens. Actuators, B* **2014**, *197*, 292−299.
(62) Santhiago, M.; Vieira, I. C. L-Cysteine Determination in Pharmaceutical Formulations Using a Biosensor Based on Laccase from *Aspergillus oryzae*. *Sens. Actuators, B* **2007**, *128*, 279−285.
(63) Wang, K.; Tang, J.; Zhang, Z.; Gao, Y.; Chen, G. Laccase on Black Pearl 2000 Modified Glassy Carbon Electrode: Characterization of Direct Electron Transfer and Biological Sensing Properties for Pyrocatechol. *Electrochim. Acta* **2012**, *70*, 112−117.
(64) Gomes, S. A. S. S.; Nogueira, J. M. F.; Rebelo, M. J. F. An Amperometric Biosensor for Polyphenolic Compounds in Red Wine. *Biosens. Bioelectron.* **2004**, *20*, 1211−1216.
(65) Shimomura, T.; Itoh, T.; Sumiya, T.; Hanaoka, T.; Mizukami, F.; Ono, M. Amperometric Detection of Phenolic Compounds with Enzyme Immobilized in Mesoporous Silica Prepared by Electrophoretic Deposition. *Sens. Actuators, B* **2011**, *153*, 361−368.
(66) Gomes, S. A. S. S.; Rebelo, M. J. F. A New Laccase Biosensor for Polyphenols Determination. *Sensors* **2003**, *3*, 166−175.
(67) Portaccio, M.; Di Martino, S.; Maiuri, P.; Durante, D.; De Luca, P.; Lepore, M.; Bencivenga, U.; Rossi, S.; De Maio, A.; Mita, D. G. Biosensors for Phenolic Compounds: The Catechol as a Substrate Model. *J. Mol. Catal. B: Enzym.* **2006**, *41*, 97−102.
(68) Xu, X.; Lu, P.; Zhou, Y.; Zhao, Z.; Guo, M. Laccase Immobilized on Methylene Blue Modified Mesoporous Silica MCM-41/PVA. *Mater. Sci. Eng., C* **2009**, *29*, 2160−2164.

DOI: 10.1021/acsami.5b04967
ACS Appl. Mater. Interfaces 2015, 7, 20612−20622